JOURNAL OF MATERIALS SCIENCE 26 (1991) 67–74

The influence of polyacrylic acid molecular weight on the fracture of zinc polycarboxylate cements

R. G. HILL, S. A. LABOK
School of Materials Science and Physics, Thames Polytechnic, Wellington Street, Woolwich, London SE18 6PF, UK

Failure in zinc polycarboxylate cements has been studied using a linear elastic fracture mechanics approach. The toughness, fracture toughness, and flexural strength increase with the poly(acrylic acid) chain length. The dependence of toughness on the poly(acrylic acid) molecular weight is not as large as predicted by a chain pull-out model for fracture. The poly(acrylic acid) chain length has a more pronounced effect than with the related glass–polyalkenoate cement, indicating that the cross-links between the chains are weaker in these cements.

1. Introduction

Zinc Polycarboxylate cements were invented by Smith [1] in 1968. They are currently used as a dental filling material and as an adhesive in the placement of crowns. Recently, they have been developed for application as a zinc-rich paint for corrosion protection [2]. In all three applications, the cement suffers from being brittle and having a low flexural strength. The present study looks at the fracture of zinc polycarboxylate cements with the aim of understanding the failure mechanism.

Despite the fact that zinc polycarboxylate cements have existed for almost twenty years, little is known about their setting reaction and final structure. Very few studies [3–5] have been undertaken and the results have often been inconclusive.

The cement is formed as a result of an acid–base reaction between a concentrated aqueous poly(acrylic acid) solution and a modified zinc oxide powder. The zinc oxide is chemically modified by reaction with small amounts of metal oxides, principally magnesium oxide at 1100 to 1200 °C; this process reduces the reactivity of the zinc oxide towards acid attack [6] and facilitates cement formation. The set cement consists of unreacted metal oxide particles embedded in a zinc polyacrylate matrix (Fig. 1). The zinc ions released from the zinc oxide particles cross-link the poly(acrylic acid) chains and effectively render them insoluble. The initial chemical studies using infrared spectroscopy indicated the cross-links formed between the zinc ions and the carboxylate groups were purely ionic. More recently, an infrared study on zinc polyacrylate [7] concluded the zinc ions were site-bound to carboxylate groups, via partially covalent bonds. A further study on the zinc oxide–poly(acrylic acid) cement system [8] concluded that whilst prior to setting the bonding was largely ionic, the set cement was bonded by zinc carboxylate complexes that have a covalent character. Therefore, we would expect zinc polycarboxylate cements to differ in their behaviour from the related glass–polyalkenoate cements. These latter materials consist of glass particles embedded in a matrix formed from anionic polyacrylate chains and either calcium ions or complex fluoro-aluminium ions of the type AlF^{2+}. In both cases the cross-links are thought to be purely ionic.

A recent fracture study [9] of glass–polyalkenoate cements has emphasized their polymeric character and has shown the toughness, fracture toughness and flexural strength of these cements to increase with the poly(acrylic acid) chain length. Furthermore, these cements exhibit sharp loss peaks, by both dielectric thermal analysis and dynamic mechanical thermal analysis that are typical of thermoplastics [10].

The sharp loss peaks correspond to the glass transition and indicate that the ionic cross-links between the poly(acrylic acid) chains must be thermally labile; therefore, these cements may be regarded as thermoplastic polymer composites. This is in marked contrast

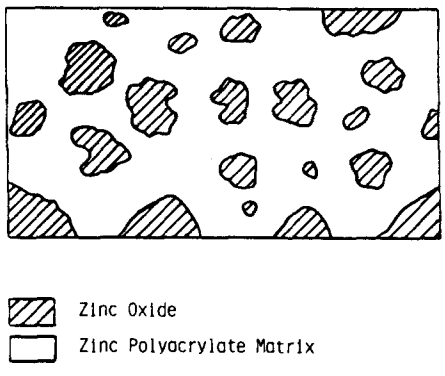

Figure 1 Schematic illustration of a zinc polycarboxylate cement showing zinc oxide particles embedded in a zinc polyacrylate matrix.

0022–2461/91 $03.00 + .12

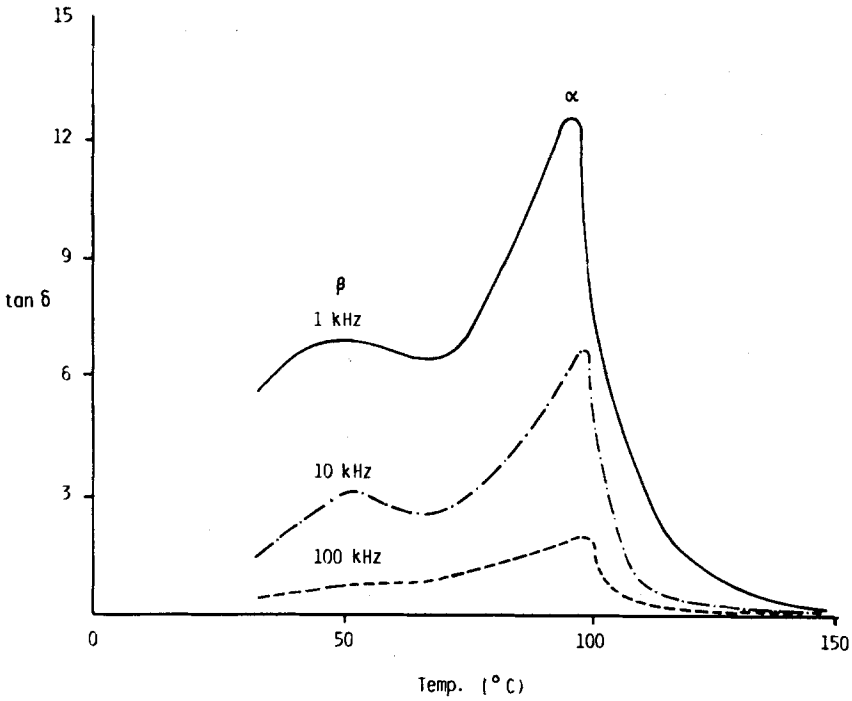

Figure 2 The dissipation factor, tan δ, at three different frequencies as a function of temperature for a zinc polycarboxylate cement.

to two previous studies [11, 12] which treated these cements as being thermosets. Although the cross-links may be reasonably stable at room temperature and slightly above, localized dilational stresses at the crack tip may well serve to break the ionic bonds and lower the effective glass transition temperature, thus allowing limited plastic flow during fracture.

Zinc polycarboxylate cements similarly show sharp loss peaks [10]; an example is shown in Fig. 2. It is therefore reasonable to expect these cements to behave in some respects like thermoplastic polymer composites.

2. Polymer fracture

Our understanding of the fracture of thermoplastic polymers is well advanced. Berry's pioneering work [13, 14] on poly(methyl methacrylate) and polystyrene demonstrated that the measured fracture surface energy of a polymer was much greater than the energy required to break all the polymer chains crossing the fracture plane. The high fracture surface energy was attributed to localized plastic flow of the polymer chains at the crack tip. Berry also attributed the inherent Griffith flaw size to a plastic zone or craze that formed just prior to catastrophic failure.

Amorphous thermoplastic polymers generally exist in the random coil conformation in the glassy state, thus during deformation and fracture the chains have to be stretched prior to any chain scission occurring. Clearly for this process to take place the chains must be held securely.

There is general recognition that the strength of high polymers is related to long-range entanglements which were viewed originally as physical knots. However, most polymer chains are too inflexible to form a physical knot. The current model [15] views a chain as being trapped in a tube of entanglements formed from neighbouring chains. This model is known as the reptation model and is shown schematically in Fig. 3.

In the reptation model a polymer chain is viewed as moving along an imaginary "tube" in a snake like fashion. The directional mobility of the chain is constricted by the entanglements forming its tube. Longitudinal motion is also restricted by the interaction of the chain with substituent groups of neighbouring chains, that give rise to potential energy barriers to chain mobility along the tube.

The reptation model has been one of the most successful models in polymer physics [16] and has been used to describe the dynamics of polymer chains [17] in melts and concentrated solutions [18] as well as fracture [19, 20] and crack healing [21]. The reptation chain pull-out model for fracture is shown in Fig. 4.

The following analysis is based on that proposed by Prentice [19]. Using a simple power law viscous model it can be shown that the shear stress (τ) experienced by the chain in its tube will be proportional to the apparent strain rate, γ_a.

$$\tau = \mu(\gamma_a)^n \tag{1}$$

where μ is a coefficient of friction resulting from the interaction between substituents on the extracted chain and the chains forming the tube. However

$$\tau = \frac{F}{A_s} \tag{2}$$

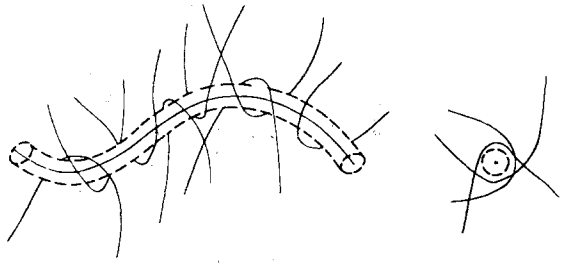

Figure 3 Schematic illustration of a polymer chain trapped in a tube of entanglements.

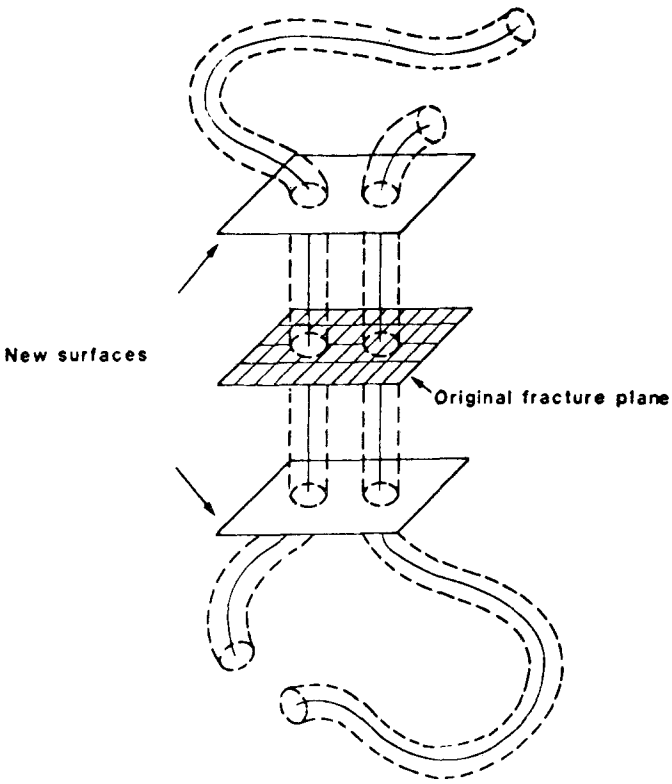

Figure 4 The reptation chain pull-out model for fracture.

where F is the force acting on the end of the chain in the direction of the tube and A_s is the effective surface area of the tube occupied by the polymer chain.

$$A_s = 2\pi rl \tag{3}$$

where r is the radius of the polymer chain, and l is the contour length of the tube occupied by the polymer molecule.

The apparent strain rate may be defined by

$$\gamma_a = \frac{V}{h} \tag{4}$$

where h is the spatial gap between the chain and the surface of its imaginary tube, and V is the rate of removal of the chain.

Combining Equations 1 to 4 we obtain

$$F = \mu 2\pi r \left[\frac{V}{h}\right]^n l \tag{5}$$

The energy to extricate one chain from its tube is then

$$\tau_o = \int_{l=0}^{l=L} F\,dl \tag{6}$$

where L is the total contour length of the tube vacated, thus

$$\tau_o = \int_{l=0}^{l=L} \mu 2\pi r \left[\frac{V}{h}\right]^n l\,dl \tag{7}$$

At constant V

$$\tau_o = \mu\pi r \left[\frac{V}{h}\right]^n L^2 \tag{8}$$

The fracture surface energy per unit area of fracture plane will then be

$$\tau = \tau_o N_s \tag{9}$$

where N_s is the number of segments crossing a unit area of crack plane. The assumption is that N_s is inversely proportional to the molecular cross-sectional area only. This assumption implies that a polymer chain only crosses the fracture plane once, which may be questionable, but considerably simplifies the analysis.

Combining Equations 8 and 9

$$\tau = \mu\pi r N_s \left[\frac{V}{h}\right]^n L^2 \tag{10}$$

The equation implies that at a fixed crack opening velocity (V) the work done in removing chains from a unit area of crack plane is proportional to the molecular weight squared.

$$\tau \propto M^2 \tag{11}$$

At some stage a molecular weight will be reached where the stress to extricate a chain from its tube is greater than that required for homolytic chain scission of an extended segment.

A result of Equation 5 is that at a constant crack opening velocity a critical value of the force (F_c) will be reached at a critical chain length (l_c). Above this value of l_c the force required to pull out chains from their tubes will be greater than that to break the carbon–carbon bonds of the polymer backbone. Below this critical value (l_c) chain pull out will be the dominant mechanism and the fracture surface energy will be determined by Equation 10, whilst above l_c, chain scission will occur and the fracture surface energy will then be independent of molecular weight.

There is also a critical chain length required in order to form entanglements. Below this chain length it will be impossible to form entanglements and as a result the reptation model will no longer apply. Typically, this critical entanglement molecular weight corresponds to between 100 and 300 monomer units.

TABLE I Molecular weight details determined by gel permeation chromatography of polyacrylic acids

Code	Batch no.	$\bar{M}_n$	$\bar{M}_w$	PD	$\bar{M}_z$
E5	159	7.30×10^3	1.15×10^4	1.58	1.69×10^4
E7	AVS 228	1.13×10^4	2.27×10^4	2.01	5.93×10^4
E9	220	4.04×10^4	1.14×10^5	2.82	2.31×10^5
E11	415	1.12×10^5	3.83×10^5	3.42	6.13×10^5

PD = polymer dispersity.

Early studies by Smith [23] showed the flexural strength of zinc polycarboxylate cements to be influenced by the poly(acrylic acid) molecular weight. These results could arise from a reduction in the inherent Griffith flaw size, possibly as a result of a reduced maximum pore size, rather than an increase in the toughness.

The present paper investigates the role of poly(acrylic acid) molecular weight on the properties of a fixed composition zinc polycarboxylate cement. The results are subsequently compared with a recent study of glass polyalkenoate cements.

3. Experimental procedure

3.1. Materials

The zinc oxide powder was a commercial material supplied by Dentsply (Addlestone, Weybridge, UK). The poly(acrylic acids) were obtained from Allied Colloids (Bradford, UK). The poly(acrylic acids) were supplied as solutions which were freeze dried to constant weight then ground in a coffee grinder. The fraction that passed through a 106 μm sieve was used in the preparation of the cements.

The poly(acrylic acids) were characterized by gel permeation chromatography using 0.1 N sodium sulphate as the eluant and polyethylene oxide molecular weight standards. The molecular weight details are listed in Table I.

3.2. Preparation of cement

Through the course of these studies, the cements were mixed at a fixed composition. The powdered poly(acrylic acid) was first blended with the zinc oxide powder in the required proportion. The cement is formed by mixing this blend with water. Typically 7 g poly(acrylic acid) were blended with 50 g zinc oxide powder.

Portions of this mixture (15 g) were then mixed with 5.0 ml distilled water to make one double torsion specimen. A smaller amount of material was mixed for the compact tension specimens, with only 7.5 g (poly-acrylic acid)/zinc oxide mixture and 2.5 ml water being required.

After mixing, the cement pastes were packed into appropriate sized moulds consisting of stainless steel plates and PTFE formers. A thin polyester film was layered over the stainless steel plates to prevent adhesion of the cement. The moulds were squeezed together using G clamps and excess cement paste eliminated. The cements were left in the mould for 1 h to allow their strength to develop sufficiently. The set specimen blanks were then removed from the mould and stored in distilled water at 37 °C for 48 ± 2 h prior to testing.

3.3. Test methods

3.3.1. The double torsion (DT) test

The double torsion test [24] has many advantages over other fracture toughness specimen geometries. The crack length is not required in the calculation of the stress intensity factor. It can be used to investigate crack stability in a material, enabling an insight into the fracture process. Providing cracks are stable the testpiece can be used to obtain crack velocity/stress intensity factor diagrams, from which static fatigue lifetimes can be predicted. The crack propagates at constant velocity down the DT specimen, the velocity being determined by the cross-head displacement rate, the specimen dimensions and the modulus of the material. The specimens are easy to manufacture and blunt cracks can readily be detected. Finally, after fracturing, the large DT specimens can be cut down to make three-point bend specimens, making economical use of materials and resources.

Double torsion specimens 75 mm × 3.5 mm × 25 mm, Fig. 5, were produced as described previously in the form of rectangular plates. A sharp groove 0.5 mm deep was cut down the centre of the specimen using a microslice cutter (Microslice II, Metals Research Ltd, Cambridge, UK). A slot was cut at one end of the specimen into which was pressed a scalpel blade.

The DT test was performed using a J. J. Lloyd (Warsash, Southampton, UK) electromechanical testing machine. During the test the specimen was supported on two parallel rollers of 3 mm diameter and spaced 20 mm apart. The load was applied at a constant rate (0.5 mm min^{-1}) to the slotted end via two 3 mm diameter ball bearings. The specimen was therefore subjected to four-point bend loading, during which the crack initiated and propagated, along the centre of the specimen, within the groove. The test was carried out in tap water at 19 ± 2 °C.

In a DT test the mode 1 stress intensity factor, K_1, is given by [25]

$$K_1 = P_c W_m \left[\frac{3(1 + \nu)}{W t^3 t_n}\right]^{1/2} \quad (12)$$

where W_m is the moment arm, W the specimen width, t the specimen thickness, t_n is the thickness in the crack plate, and ν is Poisson's ratio (assume to be

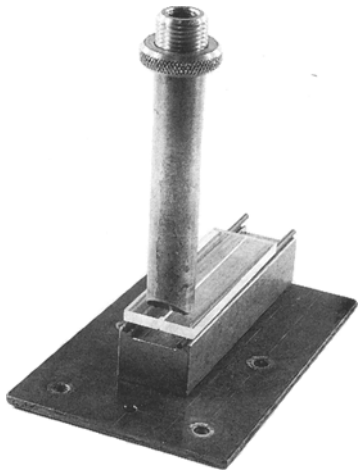

Figure 5 The double torsion (DT) specimen and test jig.

0.33). Values for K_1 (the fracture toughness) were obtained by substituting the appropriate specimen dimensions along with the load at fracture P_c into Equation 12. A typical load/deflection plot is shown in Fig. 6 for stable crack growth.

3.3.2. The compact tension test

The compact tension test piece was a miniature version of the one described in BS 5447 [26]. The value of W was reduced to 20 mm and the specimen thickness was reduced from $0.5W$ to $0.3W$ (Fig. 7).

The specimen blanks were cut along the dashed line (Fig. 8) using an edge-coated diamond flitting wheel, such that the final length of the sawcut was between $0.45W$ and $0.55W$. The length of the fine sawcuts were measured prior to testing. The specimens were then tested quasi-statistically in a J. J. Lloyd testing machine using a cross-head velocity of 0.5 mm min^{-1}. All tests were carried out in tap water at 19 $\pm$ 2 °C. The Gurney–Hunt Sector [27] area method could not be applied due to the opacity of the cements. Instead the total area under the curve was used to calculate the toughness (G_1). A typical load–deflection record for a compact tension specimen is shown in Fig. 8.

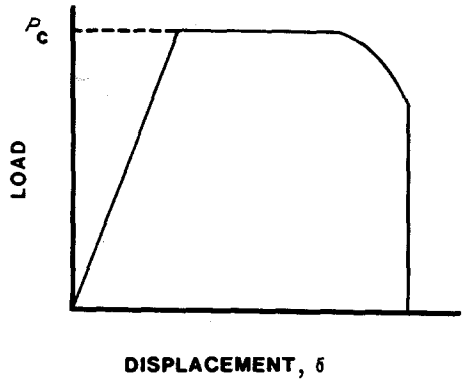

Figure 6 A typical load–deflection plot for a DT specimen undergoing stable crack growth.

The maximum load at fracture (P_c) and the sawcut length (a) were substituted into Equation 12 to give the mode 1 stress intensity factor (K_1).

$$K_1 = \frac{P_c}{tW^{1/2}}(Y) \quad (13)$$

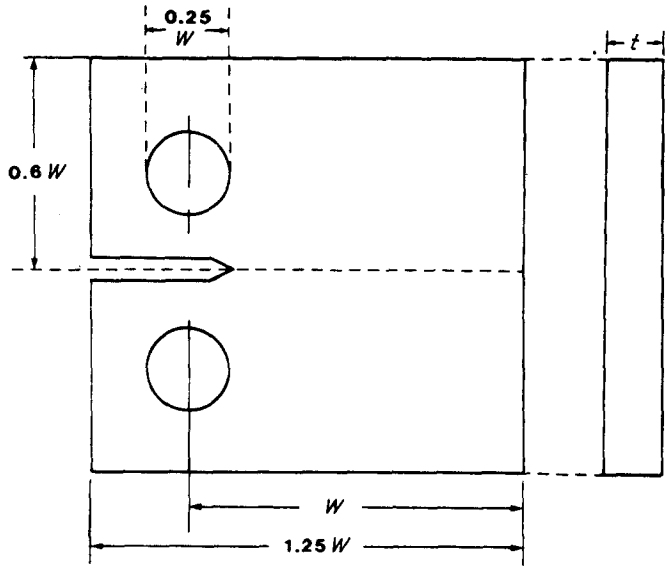

Figure 7 A compact tension (CT) specimen.

TABLE II The influence of poly(acrylic acid) molecular weight on fracture toughness, toughness and flaw size

Code	$\bar{M}_w$	DT values				CT values			
		K_1 (MN m$^{-3/2}$)	SD ($n = 5$)	G_1 (J m^{-2})	a^* (mm)	K_1 (MN m$^{-3/2}$)	SD ($n = 5$)	G_1 (J m^{-2})	a^* (mm)
E5	1.15×10^4	0.21	0.02	10	0.58	0.22	0.04	12	0.60
E7	2.27×10^4	0.46	0.08	31	1.12	0.37	0.06	36	0.72
E9	1.14×10^5	0.61	0.17	67	0.87	0.53	0.09	74	0.65
E11	3.83×10^5	0.80	0.12	115	1.40	0.67	0.09	129	0.98

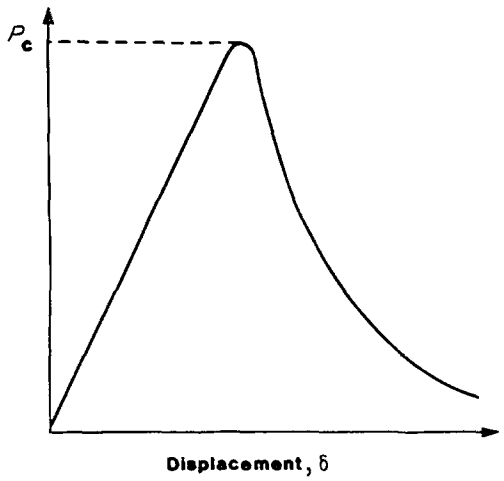

Figure 8 A typical load–deflection plot for a CT specimen.

where

$$Y = 29.6\left(\frac{a}{W}\right)^{1/2} - 185.5\left(\frac{a}{W}\right)^{3/2} + 655.7\left(\frac{a}{W}\right)^{5/2} - 1017\left(\frac{a}{W}\right)^{7/2} + 638.9\left(\frac{a}{W}\right)^{9/2} \quad (14)$$

3.3.3. The flexural test

Immediately after testing the DT specimens, the broken halves were cut up into three-point bend specimens, measuring 75 mm × 3.5 mm × 10 mm. In a three-point bend specimen the relationship between the applied load (p) and the deflection at the centre of the specimen (s) for a specimen of rectangular cross-section is given by

$$p = \frac{4\delta Ebt^3}{s^3} \quad (15)$$

where t is the beam thickness, b is the beam width, s is the span. A span of 20 mm was used, with a cross-head displacement rate of 5.0 mm min^{-1}. This gives a similar strain rate to that used in the DT tests. All tests were carried out in tap water at 20 ± 2 °C. The Young's modulus was calculated from the initial tangent of the load–deflection plot. The unnotched fracture strength was defined by

$$\sigma_f = \frac{3Ps}{2bt^2} \quad (16)$$

A minimum of five specimens were tested for each test condition.

3.3.4. Calculation of the strain energy release rate (G_1) from DT specimens

The strain energy release rate was calculated assuming that pure linear elastic fracture mechanics apply using the following expression

$$G_1 = \frac{K_1^2}{E} \quad (17)$$

3.3.5. Calculation of the Griffith flaw size

A linear elastic fracture mechanics approach was used to calculate the inherent flaw size. This value estimates the size of microstructural features, or defects which limit the strength of the material in the absence of an external crack. Sharp flaws larger than the inherent flaw size will generally reduce the strength of the material. The method used for the calculation of the inherent flaw size is based on the Irwin relation, which is applicable to the geometry and loading of a bend-type single-edge notch specimen first used by Brown and Strawley [28]

$$K_1 = Y\frac{6m}{tw^2}(a)^{0.5} \quad (18)$$

where m is the bending moment equal to $Ps/4$ and Y is a geometrical calibration factor, which in the absence of an external crack, assumes a value of 1.93.

The Irwin relation can be written in terms of the fracture toughness (K_1): the unnotched fracture strength (σ_f) and the flaw size (a^*)

$$a^* = \left(\frac{K_1}{Y\sigma_f}\right)^2 \quad (19)$$

4. Results and discussion

All the cements underwent slow stable crack growth in the two fracture toughness tests. There was no evidence of any plastic deformation in the flexural tests. There is good agreement between the double torsion and the compact tension data (Table II), both for the stress intensity factor and the toughness. Linear regression analysis gave correlation coefficients of 0.994 and 0.999, respectively, for fracture toughness and toughness data. This provides strong evidence for the validity of the data and for the application of linear elastic fracture mechanics to these cements.

The fracture toughness and toughness, both increase with the poly(acrylic acid) (PAA) chain length. The magnitude of the increase is greater than with the

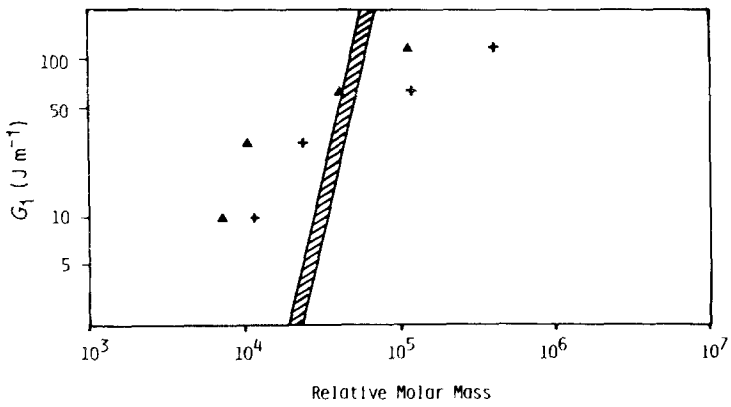

Figure 9 A plot of log(toughness) against (▲) log($\bar{M}_n$) and (+) log($\bar{M}_w$). The shaded line indicates the slope predicted from the reptation chain pull-out model for fracture.

related glass–polyalkenoate cements. $\text{Log}_{10}G_1$ is plotted against $\log_{10}$ (molar mass) in Fig. 9; the toughness is clearly not proportional to the molecular mass squared, predicted from the chain pull-out model for fracture. The slope of approximately 1.0 is, however, closer to the theoretical value of 2.0 than with the related glass polyalkenoate cements, where the slope is about 0.5.

It is possible that the larger influence of PAA chain length with the zinc polycarboxylate cements reflects a more thermoplastic character as a result of weaker linkages between the polymer chains. Stress relaxation studies [29, 30] provide some support for the cross-links in zinc polycarboxylate cements being more labile than in the related glass polyalkenoate cements. Unlike the glass polyalkenoate cements, the Young's modulus (Table III) is not independent of the poly(acrylic acid) chain length, the cement made with the lowest molecular weight polyacid, exhibits a significantly lower modulus than the other cements. The modulus would be expected to be constant for a fixed chemical composition. The reduction in Young's modulus found for the lowest molecular weight cement probably reflects the influence of free volume at low molecular weights.

The glass transition is conventionally [31] given by

$$T_g = T_{g\infty} - \frac{K}{\bar{M}_n}$$

where T_g is the glass transition temperature, $T_{g\infty}$ is the glass transition temperature for an infinitely long polymer chain, K is a constant, and $\bar{M}_n$ is the number average molecular weight.

At very high molecular weights, large values of $\bar{M}_n$, the glass transition temperature, T_g, will approach $T_{g\infty}$. At low molecular weights the glass transition temperature will deviate significantly from $T_{g\infty}$ and as a result of this the Young's modulus will also be lower.

TABLE III The influence of PAA molecular weight on flexural strength and Young's modulus

Code	$\bar{M}_w$	σ_f (MN m^{-2})	SD ($n = 5$)	E (MN m^{-2})	SD ($n = 5$)
E5	1.15×10^4	4.65	0.28	4439	372
E7	2.27×10^4	7.13	1.26	6611	675
E9	1.14×10^5	10.74	0.36	5622	429
E11	3.83×10^5	11.08	1.14	5580	520

For this effect to occur the degree of cross-linking in the cement must be very low, such that the polymer chains, or a significant proportion of them, act as individual chains. Thus, the modulus data support the concept of the chains being less tightly cross-linked than in the glass–polyalkenoate cements where there is no reduction in the Young's modulus on reducing the PAA molecular weight.

The flexural strength (Table III) increases with the polyacid molecular weight from 4.65 MPa at $\bar{M}_n = 1.15 \times 10^4$ to 11.08 MPa at $\bar{M}_n = 3.83 \times 10^5$. This increase in the flexural strength is largely a result of the increase in the toughness. The inherent flaw size (a^*) does not vary systematically with molecular weight but is thought to correspond to macroscopic pores, or surface cracks, because these cements are more porous and have a poor surface finish compared with the glass–polyalkenoate cements.

In the glass–polyalkenoate cements the inherent flaw size varied with the molecular weight of the polyacid suggesting that the flaw size corresponded to a plastic zone, or craze that forms just prior to fracture.

The large inherent flaws present result in the flexural strength of zinc polycarboxylate cements being comparable to glass–polyalkenoate cements, despite their superior fracture toughness.

5. Conclusions

The chain length of the poly(acrylic acid) has a significant influence on the fracture properties, toughness, fracture toughness and flexural strength of zinc polycarboxylate cements. These unusual cements behave in many respects like thermoplastic polymer composites. The cross-links between the chains appear to be weaker than in the glass–polyalkenoate cements, which is at variance with the conclusions from infrared spectroscopy studies which implied that the cross-links are largely covalent in zinc polycarboxylate cements. The fracture data support the view proposed by Paddon and Wilson [29] that the polymer chains in these cements can slip past one another and that therefore the cross-links between the chains must be relatively weak. In conclusion, it may be better to treat the linkages between the chains, not as cross-links, but as interchain attractions. These interchain attractions are probably sufficiently strong to cause chain scission at modest molecular weights ($< 10^5$) and hence the

chain pull-out model does not apply quantitatively to these cements.

Acknowledgements

The authors thank Dr J. Nicholson, Laboratory of the Government Chemist, for copies of papers prior to publication, and to Dentsply Ltd for the supply of the cement powder.

References

1. D. C. SMITH, *Br. Dent. J.* **125** (1968) 381.
2. A. D. WILSON, H. J. PROSSER, J. C. SKINNER and A. J. DUNSDON, UK Pat. Appl. **84**, 27 138 (1984).
3. S. CRISP, H. J. PROSSER and A. D. WILSON, *J. Mater. Sci.* **11** (1976) 36.
4. A. D. WILSON, *J. Biomed. Mater. Res.* **16** (1982) 544.
5. M. A. MOHARRAN, H. ABDEL-HAKEEN, H. SHAHEEN and R. M. IBRAHIM, *J. Mater. Sci.* **21** (1986) 1681.
6. A. D. WILSON, *Chem. Soc. Rev.* **7** (1975) 254.
7. J. W. NICHOLSON and A. D. WILSON, *Br. Polym. J.* **19** (1987) 67.
8. J. W. NICHOLSON, O. M. LACY, G. S. SAYERS and A. D. WILSON, *J. Dent. Res.* **22** (1988) 623.
9. R. G. HILL, C. P. WARRENS and A. D. WILSON, *J. Mater. Sci.* **24** (1989) 363.
10. R. G. HILL, *J. Mater. Sci. Lett.* **8** (1989) 1043.
11. M. J. READ and K. A. HODD, *Adhesives*, **8** (1984) 153.
12. M. J. READ, PhD thesis, University of Brunel (1974).
13. J. P. BERRY, *J. Polym. Sci.* **50** (1961) 1.
14. J. P. BERRY, *S.P.E. Trans.* **1** (1961) 1.
15. S. F. EDWARDS, *Proc. Roy. Soc. London* **92** (1969) 9.
16. P. G. DE GENNES, *Physics Today* June (1983) 344.
17. J. KLEIN, *Nature* **271** (1978) 143.
18. M. TIRREL, *Rubber Chem. Technol.* **57** (1984) 523.
19. P. PRENTICE, *Polymer* **24** (1983) 344.
20. G. L. PITMAN and I. M. WARD, *ibid.* **20** (1979) 895.
21. K. JUD, H. H. KAUSCH and J. G. WILLIAMS, *J. Mater. Sci.* **16** (1981) 204.
22. P. PRENTICE, *ibid.* **20** (1985) 1445.
23. D. C. SMITH, *J. Canad. Dent. Assoc.* **37** (1971) 22.
24. D. P. WILLIAMS and A. G. EVANS, *J. T. Eval.* **264** (1973).
25. J. A. KIES and B. J. CLARKE, in Proceedings of the 2nd International Conference on Fracture, Brighton, April 1969, edited by P. L. Pratt (Chapman and Hall, London, 1969) p. 483.
26. BS5447, "Plane strain crack toughness K_{IC} Testing of Metallic Materials" (British Standards Institution, London, 1977).
27. C. GURNEY and J. HUNT, *Proc. Roy. Soc. London* **A299** (1967) 508.
28. W. F. BROWN and J. E. STRAWLEY, "Plane strain crack toughness testing on high strength metallic materials", ASTMS STP 410 (American Society for Testing and Materials, Philadelphia, Pennsylvania, 1965) p. 13.
29. J. M. PADDON and A. D. WILSON, *J. Dent.* **4** (1976) 183.
30. S. CRISP and A. D. WILSON, *Br. Polym. J.* **7** (1975) 279.
31. R. J. YOUNG, in "Introduction to Polymers" (Chapman and Hall, London, 1981) p. 204.

Received 13 June
and accepted 8 November 1989